JOURNAL OF MATERIALS SCIENCE 24 (1989) 1853–1861

Dense single-phase β-sialon ceramics by glass-encapsulated hot isostatic pressing

THOMMY EKSTRÖM
AB Sandvik Hard Materials, P.O. Box 42056, S-126 12 Stockholm, Sweden
P. O. KÄLL, MATS NYGREN, P. O. OLSSON
University of Stockholm, Department of Inorganic Chemistry, Arrhenius Laboratory, S-106 91 Stockholm, Sweden

Single phase β-sialon ceramics, $Si_{6-z}Al_zO_zN_{8-z}$, have been prepared from carefully balanced powder mixtures, also taking account of any excess oxygen in the starting materials. Sintering powder compacts in a nitrogen atmosphere (0.1 MPa) at 1800° C or higher transforms the starting mixture into a β-sialon solid solution at z-values up to about 4.3, but the sintered material has an open porosity. Addition of 1 wt% Y_2O_3 to the starting mix improved the sintering behaviour somewhat and the density of the sintered compacts reached 95% of the theoretical value. By glass-encapsulated hot isostatic pressing at 1825° C, however, sintered materials of virtually theoretical density could be obtained, with or without the 1 wt% Y_2O_3 addition. These latter samples have been studied by X-ray diffraction and electron microscopy, and their hardness and indentation fracture toughness have been measured. It was found that the maximum extension of the β-sialon phase composition at 1825° C and 200 MPa pressure is slightly below 4, $z \sim 3.85$ and about 4.1 at atmospheric pressure, and that the hexagonal unit cell parameters are linear functions of the z-value. The single-phase β-sialon ceramics had no residual glassy grain-boundary phase. The grain shape was equi-axed and the grain size increased from about 1 μm at low z-values to 5 μm at high z-values. At low z-values the hardness at a 98 N load was 1700 and the fracture toughness 3, whereas an increase in z above 1 caused both the hardness and fracture toughness to decrease significantly. Addition of 1 wt% Y_2O_3 to the starting mix prior to the HIP-sintering gave rise to a small amount of amorphous intergranular phase, changes in grain size and shape, a clear increase in fracture toughness and a moderate decrease in hardness.

1. Introduction

An extensive body of information on silicon nitride based ceramics has been generated during the last 15 years, with interest increasingly directed towards the so-called sialon ceramics. The first work on solid solutions in the system silicon nitride–aluminum oxide was performed independently by Jack and Wilson [1] and by Oyama and Kamigiato [2]. A solid solution $Si_{6-z}Al_zO_zN_{8-z}$, formed by the simultaneous substitution of Al and O for Si and N, respectively, in Si_3N_4 gives an expanded β-Si_3N_4 lattice. This solid solution was called β-sialon, an acronym for Si–Al–O–N. One of the problems in the densification of silicon nitride is posed by the low diffusion rates which make the process very difficult. Thus, addition of Al_2O_3/AlN mixtures will not normally enable pressureless sintering to near-theoretical density unless special precautions are taken in the processing [3, 4]. Most high-density β-sialon materials reported, made by Al_2O_3/AlN addition only, are either hot pressed [5] or sintered at high temperatures (1800 to 2000° C) under high pressure of nitrogen gas to prevent decomposition of silicon nitride [6]. Also, in these materials a liquid-phase sintering mechanism is important for the densification, compensating for the low diffusion rate in solid Si_3N_4. It is well known that the commercially available Si_3N_4 raw materials contain some oxygen that is present as a thin silica or silicon oxynitride layer on the particles [7]. Added alumina will react with this layer to form a viscous Si–Al–O–N liquid phase at the sintering temperature. Carefully balanced overall compositions, taking into account the oxygen impurity, are needed to ensure that the primary liquid phase will not remain as a residual glassy phase in the ceramic material [8].

With glass-encapsulated hot isostatic pressing (HIP) of virgin powder mixtures, silicon nitride can be densified without or with only small additions of sintering aids [9, 10]. By a combination of injection moulding and glass-encapsulated HIP, very complex shapes have been possible to fabricate [11]. Thus this processing technique is very attractive and offers a possibility to make dense β-sialon ceramics with no residual glassy grain-boundary phase and thus with better high temperature properties. It has previously been shown by Mitomo and colleagues [12] that hot-pressed β-sialon ceramics prepared from "balanced" powder mixtures, accounting and compensating for

0022–2461/89 $03.00 + .12

the surface oxides on Si_3N_4 and AlN, have better high temperature strength than similarly prepared sialon ceramics without compensation for the "excess oxygen". This paper reports the fabrication of dense β-sialon ceramics from carefully "balanced" powder mixtures without additions of other sintering aids or with only very small additions of yttrium oxide (1 wt %). The obtained materials have been carefully characterized by X-ray diffraction and electron microscopy techniques, and some physical properties have been measured.

2. Materials and experimental procedure

The samples manufactured for this study corresponded to pure β-sialon ceramics $Si_{6-z}Al_zO_zN_{8-z}$ or similar compositions with 1 wt % Y_2O_3 added. Samples with z = 0.25, 0.35, 0.50, 0.75, 1.50, 2.00, 3.00, 4.00, 4.20 and 4.50 were prepared from silicon nitride (H.C. Starck, grade LC1), aluminium nitride (H.C. Starck, grade A), aluminium oxide (Alcoa, grade A16SG) and yttrium oxide (99.9%, H.C. Starck). The oxygen contents of the silicon nitride corresponded to 2.9 wt % SiO_2, and of the aluminium nitride to 1.9 wt % Al_2O_3. This excess oxygen present in the starting materials was compensated for in the preparations. The starting materials were mixed with propanol and lubricants and vibro-milled for 16 h in sample batches of 500 g dry weight, i.e. semi-pilot-plant scale. The milling medium consisted of sialon bodies, containing 6 wt % Y_2O_3. Chemical analysis of milled sialon blends without added yttria showed that the milled-in yttrium content was well below 0.01% in all cases. Thus, virtually no material was transferred to the powder from the milling medium. After drying, disintegration of the dry powder cake and agglomeration, compacts of size 16 × 16 × 6 mm were made by die-pressing at 125 MPa. After burning off the lubricants at 600° C in a hydrogen gas flow, the powder compacts were HIP-sintered at 1825° C and 200 MPa argon pressure for 1 h, using the glass-encapsulation technique. As controls, three series of the powder compacts were also sintered in a normal fashion at 1800° C and 1850° C under atmospheric pressure (0.1 MPa) of nitrogen gas or at 1850° C under an increased nitrogen pressure of 20 MPa to prevent nitrogen losses from the specimens. The specimens were embedded in micron-sized BN powder in graphite crucibles.

To check for any compositional changes caused by the fabrication process, the dense HIP-sintered sialon materials were analysed for Si, Al, O and N and so were the powder compacts after burning off the lubricants. The results are summarized in Table I; the small deviations from the aimed-at compositions all fall within the normal errors of the methods used.

After sintering, the specimens were prepared for physical characterization by grinding and polishing, using standard techniques. X-ray diffraction analysis was performed both by diffractometry (Rigaku rotating Cu-anode, 10 kW) on polished surfaces of the sintered materials and by the Guinier-Hägg camera technique on a slice cut from the material and crushed to a powder. An internal standard substance was used, which was mixed with the powdered samples (Si with a = 0.54301 nm) or dusted on the diffractometer specimen surface (TiN with a = 0.4240 nm). The lattice parameters of the hexagonal β-sialon phase were calculated with a least-squares programme from a great number of diffraction positions. The two X-ray diffraction methods gave identical phase analysis results and lattice parameters.

TABLE I Comparison of the chemical analyses of a powder compact after the pre-sintering step and by the final dense HIP-sintered sialon materials with aimed-at compositions $Si_{6-z}Al_zO_zN_{8-z}$

Aimed z-value	Results from chemical analysis	
	Pre-sintered z	HIP-sintered z
0.25	0.29	0.26
0.35	0.39	0.35
0.50	0.53	0.49
0.75	0.78	0.79
1.50	1.51	1.53
2.00	1.99	2.00
3.00	3.02	3.01
4.00	3.98	4.04
4.20	4.19	4.20
4.50	4.48	4.48

Special care was taken when polishing the specimens for microscopy studies, fracture toughness and hardness measurements to minimize the type of compressive stress that may build up in the surface of the specimen and to minimize the material pull-out. The hardness (HV 10) and indentation fracture toughness (K_{IC}) at room temperature were obtained with a Vickers diamond indenter using a 98 N (10 kg) load. The indentation fracture toughness was evaluated with the method of Anstis and co-workers [13] after measuring the total length of the cracks emanating from the corners of the hardness impressions and assuming Young's modulus, E, to be 300 GPa.

Specimens for scanning electron microscopy (JEOL JSM 820 equipped with a Link AN 10000 EDS analyser) were studied on polished surfaces after vapour application of a carbon coating to reduce specimen charging in the electron beam. Specimens were also etched in a CF_4 plasma before the SEM studies in order to reveal the grain boundaries [14]. Specimens for transmission electron microscopy were obtained from the HIP-fabricated specimens by cutting thin slices of the material (< 0.2 mm) with a wire saw (Unipress W 520 A) and fitting them into the specimen holder by a specially designed drill. The final thinning was done by ion-milling by a 5 kV argon atom beam at an incident angle of 20°. The electron microscope used was a JEOL 200 CX, equipped with a ± 10° goniometer stage. The atomic coordinates used were those given by Van Dijen and colleagues [15]. The multislice calculations were made by a locally modified version of the SHRLI-program package [16].

3. Results

3.1. Sintering

Samples of overall compositions $Si_{6-z}Al_zO_zN_{8-z}$, with z = 0.25 to 4.5, prepared from carefully balanced powder mixtures have been sintered in this study. A second series of similar overall compositions, with

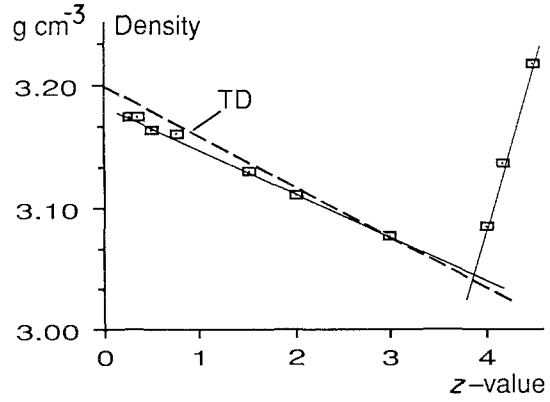

Figure 1 Densities of sialon compositions $Si_{6-z}Al_zO_zN_{8-z}$ plotted against z. All materials were glass-encapsulated HIP-sintered. The dashed curve shows the theoretical density (TD) for a single-phase β-sialon.

1 wt % of Y_2O_3 added, was also studied in order to reveal the effects of small sintering aid additions.

First a normal "pressureless" sintering was performed at 1800° C under atmospheric pressure (0.1 MPa) of nitrogen for 2 h. The pure sialon powder compacts showed no measurable shrinkage after the heat-treatment, and they had an open porosity. The weight loss for these samples was 3 to 6%. However, with only 1% yttria added to these compositions, the observed linear shrinkage varied between 5 and 15%, with the best densification noted at the compositions with $z = 1.5$ to 3; these samples had a closed porosity and a density about 93% of the theoretical (TD). The weight loss was $< 2\%$ for these latter samples.

In a second sintering experiment under atmospheric pressure of nitrogen the temperature was raised to 1850° C for 1 h. This, however, had a dramatic negative influence. Increased decomposition of silicon nitride caused weight losses of 5 to 20%, and these samples were not investigated further. Instead, a third sintering series was performed at 1850° C for 1 h, with the nitrogen gas pressure raised to 20 MPa (200 atm.). The observed weight losses then dropped below 1%. Sialon samples without Y_2O_3 addition still had an open porosity; the samples with $z \geqslant 1.5$ had started to sinter, however, and exhibited a linear shrinkage of about 5 to 10%. The yttria-containing sialon samples with $z \geqslant 1.5$ had a closed porosity and a density of about 95% TD.

TABLE II Densities (g cm^{-3}) of sialon materials made by glass-encapsulated HIP-sintering. For the single phase β-sialon ceramics, comparison is made with the calculated theoretical density.

Aimed z-value	No additions		% TD	1 wt % Y_2O_3 added
	Observed density	Theoretical density		Observed density
0.25	3.175	3.201	99.2	3.170
0.35	3.174	3.187	99.5	3.161
0.50	3.164	3.180	99.7	3.167
0.75	3.161	3.170	99.7	3.166
1.50	3.130	3.139	99.8	3.120
2.00	3.111	3.118	99.6	3.117
3.00	3.077	3.077	100.0	3.081
4.00	3.085	–	–	3.107
4.20	3.136	–	–	3.151
4.50	3.217	–	–	3.214

Finally, virgin powder compacts were glass-encapsulated and HIP-sintered at 1825° C, 200 MPa, for 1 h. All these samples showed a linear shrinkage of about 16% and a closed porosity. For the single phase β-sialon ceramics the density was in all cases above 99% TD. The measured densities given in Table II are compared with the calculated theoretical densities for the pure β-sialons using the observed lattice parameters and the molar mass. The observed density for the yttria-free sialon materials is plotted against the z value in Fig. 1. It is seen that the densities fall upon two separate straight lines intersecting at about $z = 3.85$.

3.2. X-ray diffraction analysis

Pressureless sintering at the lowest temperature, 1800° C, of low z materials without yttria left the reaction incomplete; small amounts of the starting materials could be detected by XRD besides the β-sialon phase. With the addition of 1 wt % Y_2O_3 at 1800° C or by raising the temperature to 1850° C (at 20 MPa pressure of nitrogen) the materials with $z = 0.25$ to 4.2 reacted to form single-phase β-sialons with the typical shift in cell parameters, *cf.* below. The lattice parameters of the β-sialon in the $z = 4.5$ sample was about the same as in the $z = 4.2$ sample, and in the former sample additional phases were observed, indicating a maximum extension of about 4.2. However, most attention has been given to the fully dense sialon ceramics prepared by glass-encapsulated HIP. Besides the phase analysis, carefully refined β-sialon lattice parameters have been obtained from the X-ray diffractometry runs as well as from the Guinier-Hägg data. The two data sets give practically the same linear relationship between z and the hexagonal lattice parameters (standard deviations within parentheses);

$$a = 0.7603(6) + z \cdot 0.002\,96(4)\,\text{nm}$$

$$c = 0.2907(8) + z \cdot 0.002\,55(6)\,\text{nm}$$

In Fig. 2 the cell dimensions obtained from Guinier-Hägg X-ray data are plotted as functions of the overall composition z. It is seen that there is no shift in cell dimensions above $z \sim 4$, indicating that this is the upper composition limit of the β-sialon solid solution at 1825° C and 200 MPa. In addition, the phase analyses show that the samples with $z > 4.0$ contain additional phases besides the β-sialon, *cf.* Table III. From Table III it is also seen that the addition of 1 wt % Y_2O_3 does not influence the cell dimensions calculated for the β-sialon phase, and in fact these points show a good fit to the regression lines given above.

3.3. Microstructure analysis

Only the dense HIP-sintered ceramics were chosen for the microscopy studies. In the optical microscope, the carefully polished surfaces seem to contain virtually no porosity at all. A few micropores of sizes below 5 μm and a few small inclusions of metallic appearance were observed. The inclusions were identified by the SEM-EDS analysis as iron silicides, probably formed by an enrichment of the trace impurities present in the starting materials [17].

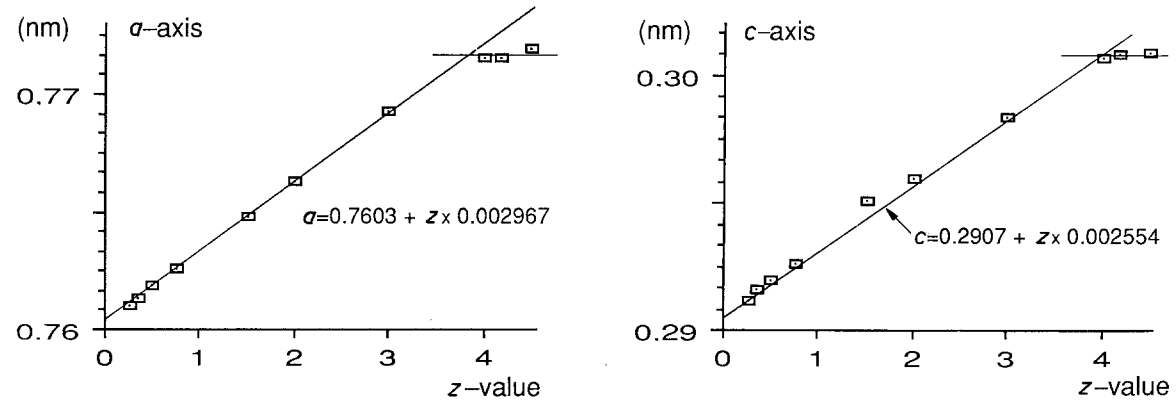

Figure 2 The unit-cell dimensions of the hexagonal β-sialon phase as functions of the z-value. Guinier-Hägg X-ray data from HIP-sintered sialon materials without yttria addition.

Direct SEM studies by secondary or back-scattered electrons could not reveal the grain structure of the sialon materials, due to the lack of contrast in the images. This was also true for the sialons with 1% yttria added. In previous studies on pressureless-sintered sialon ceramics, with higher additions of sintering aids, it has been found that etching of the specimens with a CF_4 plasma delineates grain boundaries between particles and reveals the internal structure of the sialon grains [17]. Therefore the samples in this study were also plasma-etched prior to SEM inspection, but no clear improvement of the microstructure image was achieved.

Most of the microstructural analyses have therefore been carried out on thinned ceramics by TEM techniques. Typical images of the microstructure for $z = 0.50$ and $z = 3.00$, with and without 1% Y_2O_3 addition, are shown in Figs 3a–d. The major difference between low and high z-value sialon materials is the grain size. With no extra additions, the grain size of the $z = 0.50$ materials is about 1 μm, as seen in Fig. 3a. The grains are chunky and some have typical hexagonal cross-sections. At $z = 3$, the grains are about a factor of 5 larger, but the grain morphology is unchanged. Addition of 1 wt% Y_2O_3 to the $z = 0.5$ material causes irregular grain growth, *cf.* Fig. 3b, some grains seem to grow faster, reaching 5 μm sizes and having a more elongated shape. The yttria addition to the $z = 3$ material causes a fairly coarse-grained microstructure, with up to 10 μm grams.

Another difference is the occurrence of an amorphous intergranular phase only in the yttria-containing samples. This amorphous phase is mostly found at crystal boundaries as a thin film and in 'pockets' between three or more crystals. In Figs 4a, b the $z = 0.50$ material with and without Y_2O_3 addition is shown at a somewhat higher magnification to exemplify this. Dark-field images using the amorphous diffraction ring clearly reveal that the pockets contain amorphous material, and subsequent EDS-analysis of such pockets in the SEM shows that the pockets contain an yttrium-rich phase. No pockets are seen in the single-phase β-sialon materials. However, it should be stressed that also in samples with added yttria we occasionally observed β-sialon crystals apparently in direct contact without any detectable intergranular film. One example of such a grain-boundary image at high resolution is shown in Fig. 5. Two crystals are seen along the [0 1 0] direction. The c-axes of the two crystals are not quite parallel. At one end of the grain-boundary image it is seen that the crystals meet without any intergranular phase, and the moiré pattern at the other end shows that it is two separate crystals that meet. This point will be further evaluated in a forthcoming paper [18].

Finally, it can be mentioned that structure images obtained in high resolution mode fit well with calculated images of the β-Si_3N_4 structure. A calculated image inserted in an experimental [0 0 1] image is shown in Fig. 6. The white spots seen at the centre of the indicated unit cell correspond to the characteristic tunnels in the β-sialon structure.

TABLE III A summary of the X-ray diffraction analysis of HIP-sintered sialon materials. The hexagonal lattice parameters were calculated with a least-squares program from data recorded with the Guinier-Hägg technique. Standard deviations are given in parenthesis.

Nom. z-value	No additions			1 wt % Y_2O_3 added		
	Extra phases	a-axis (nm)	c-axis (nm)	Extra phases	a-axis (nm)	c-axis (nm)
0.25	–	0.76105(4)	0.29119(3)	–	0.76101(4)	0.29131(3)
0.35	–	0.76131(4)	0.29161(2)	–	0.76118(5)	0.29182(5)
0.50	–	0.76190(3)	0.29194(2)	–	0.76186(4)	0.29191(3)
0.75	–	0.76259(6)	0.29265(4)	–	0.76280(5)	0.29260(3)
1.50	–	0.7648 (1)	0.2951 (1)	–	0.76452(6)	0.29470(7)
2.00	–	0.76631(5)	0.29592(3)	–	0.76628(5)	0.29569(3)
3.00	–	0.76927(5)	0.29835(3)	–	0.76904(5)	0.29821(3)
4.00	–	0.77155(6)	0.30069(4)	Al_2O_3	0.77150(4)	0.30060(3)
4.20	Al_2O_3 + 8H*	0.77157(5)	0.30083(4)	Al_2O_3 + 8H*	0.77163(6)	0.30086(5)
4.50	Al_2O_3 + 8H*	0.77201(7)	0.30091(5)	15R*	0.77183(6)	0.30101(4)

*8H and 15R denote the 8H and 15R sialon polytype phase, respectively.

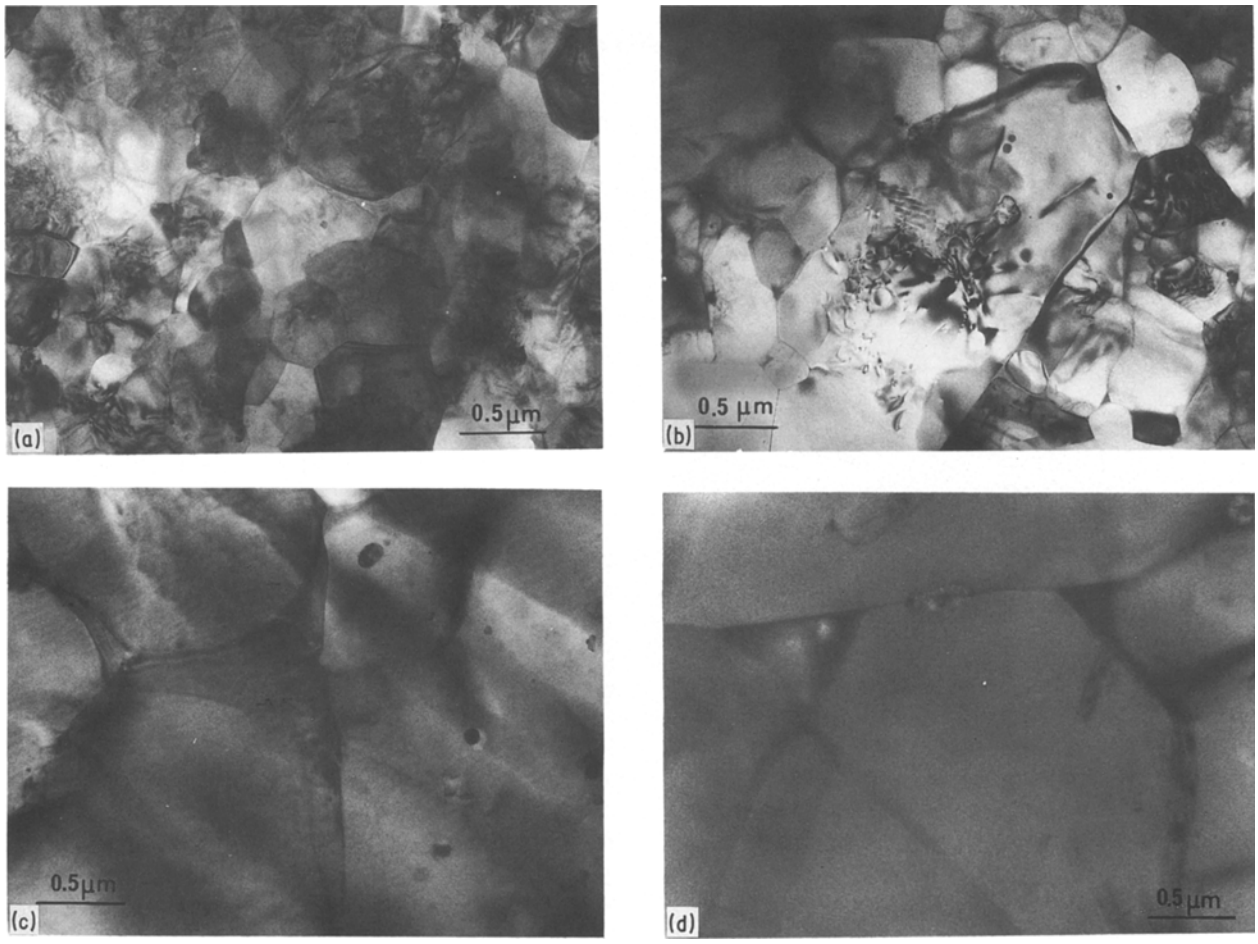

Figure 3 TEM micrographs of argon-ion thinned β-sialon samples at the same magnification, illustrating the effects on the microstructure of altering the z-value and of Y_2O_3 additions. (a) and (c) show single-phase β-sialon ceramics at $z = 0.5$ and 3, respectively, and (b) and (d) the corresponding materials with 1 wt % Y_2O_3 added.

3.4. Physical properties

The Vickers hardness ($HV10$) and the indentation fracture toughness (K_{IC}) of the HIP-sintered sialon ceramics were measured at room temperature, see Figs 7 and 8, respectively. The hardness of the single-phase β-sialon ceramics without yttria and with low z-values, i.e. close to silicon nitride, is fairly high: of the order of 1700. Increasing aluminium and oxygen substitution into β-Si_3N_4 expands the lattice, and the hardness of the single-phase β-sialon ceramics decreases slowly up to about $z = 1.5$ and then more rapidly to a minimum of about $HV10 = 1350$ at the highest substitution, about $z = 4$, see Fig. 7. In the multiphase materials formed for still higher Al_2O_3/AlN additions, the hardness increases again. The addition of 1 wt % Y_2O_3 to the material gives a significantly lower hardness at low z-values. However, the minimum hardness at about $z = 4$ is of about the same magnitude.

The fracture toughness of the low-substituted silicon nitride is about 3 and decreases slowly with increasing substitution in the single-phase β-sialon ceramic, see Fig. 8. When other phases, alumina and sialon poly-

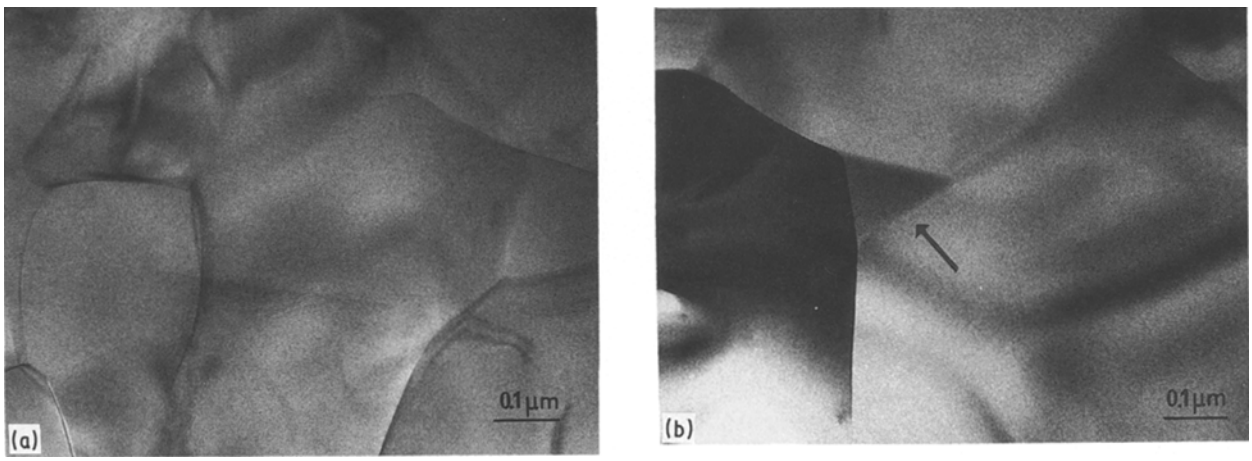

Figure 4 TEM micrographs of argon-ion thinned samples with a nominal composition corresponding to a z-value of 0.5 at a higher magnification, revealing the presence or absence of an intergranular phase. 1 wt % Y_2O_3 has been added as sintering aid to sample (b).

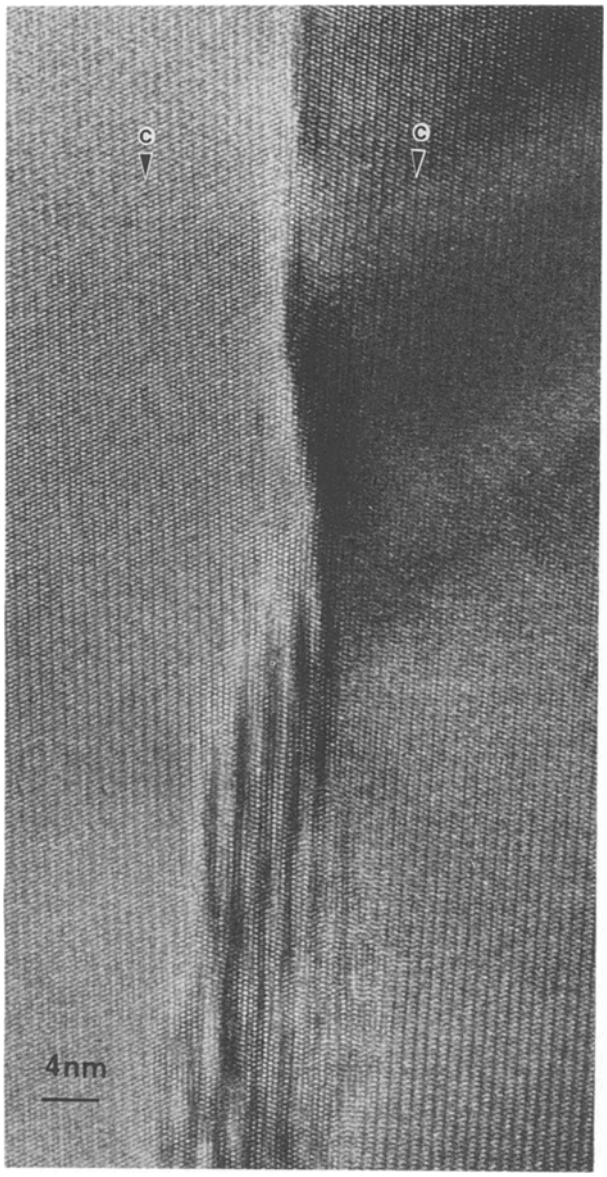

Figure 5 [1 0 0] image showing two β-sialon grains without detectable intergranular phase. Moiré fringes are visible in the lower part of the image, see text.

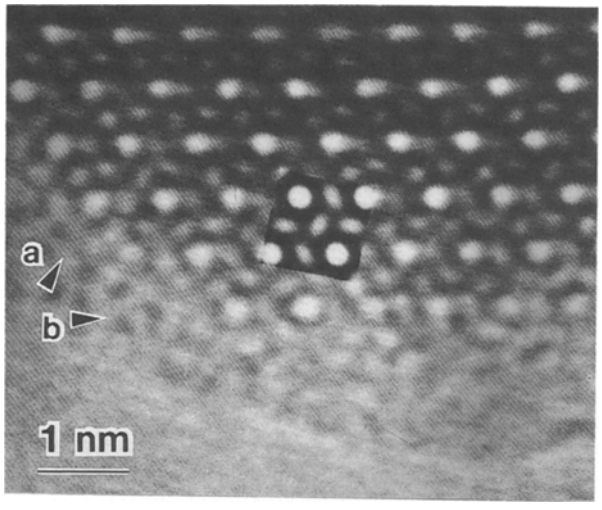

Figure 6 Calculated structural image of a β-sialon inserted into an experimental 0 0 1 image. The latter was transferred directly on-line to an image-processing system. The calculations correspond to a thickness of 4.0 nm and a defocus of -92.2 nm.

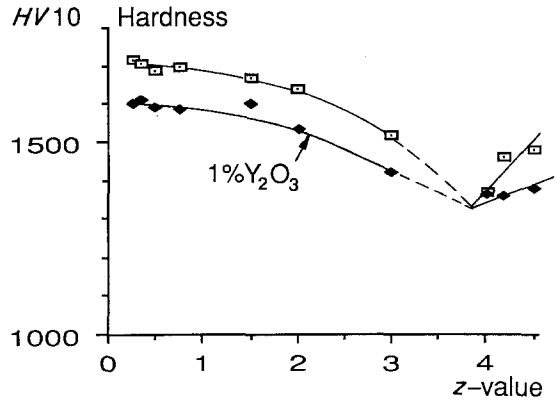

Figure 7 The measured Vickers hardness with a 98 N load ($HV10$) as a function of the z-value for the β-sialon phase, with and without 1% Y_2O_3 addition.

types, appear in the sintered ceramics, a clear rise in the fracture toughness is seen at $z \geqslant 4$. The addition of 1 wt % Y_2O_3 prior to the HIP-sintering has a dramatic effect on the fracture toughness of the sialon material, especially at low z-values, see Fig. 8. At $z = 0.25$ the fracture toughness is 4.5 and then drops with increasing z-value, but the toughness never falls below 3 at any composition.

4. Discussion

The inherent good properties of silicon nitride cannot be achieved unless the ceramic material is fabricated to near-theoretical density. In our opinion, the silicon nitride ceramics for high-performance applications should have a density of at least 99% TD, or preferably higher, and only microporosity should be allowed.

The sintering experiments in this study on β-sialon ceramics have a direct bearing on this demand for near-theoretical density. This it can be concluded that neither pressureless sintering at 1800 to 1850° C nor sintering at 1850° C under a 20 MPa nitrogen pressure are adequate production techniques. The best densities obtained which were achieved in the latter sintering, were only about 95% TD. On the other hand, glass-encapsulated HIP of balanced powder mixtures without yttria addition gave materials with densities $>99\%$ TD. In fact, these materials were so close to full density that admixture of 1 wt % Y_2O_3 as a sintering aid gave no further improvement.

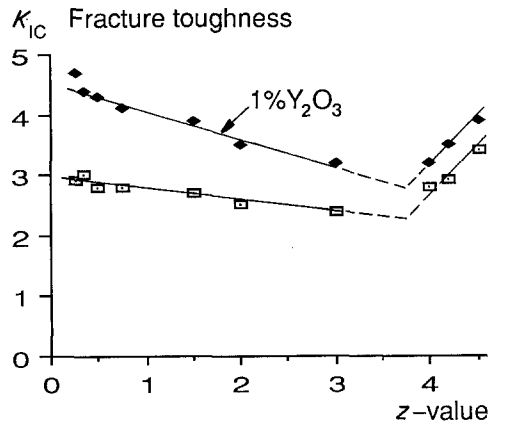

Figure 8 Measured indentation fracture toughness values (K_{IC}) plotted as a function of the composition (z-value) of the β-sialon, with and without 1% Y_2O_3.

It should, however, be stressed that it is not always easy to calculate the theoretical density for polyphasic materials. In the literature it sometimes is not clear how the TD values have been obtained for polyphase materials, as the phase amounts and densities of all constituent components have to be known. In the present investigation, besides measuring the density of the β-sialon materials, we also examined them carefully for porosity in an optical microscope.

In early sintering studies on pure β-sialon ceramics, Briggs [3] reported that he had achieved 99% TD by pressureless sintering of $Al_2O_3/AlN/Si_3N_4$ mixtures at 1740 to 1780° C. However, calculations made by us on the given amounts of mixed raw materials indicate that no account was taken of the oxygen contents of Si_3N_4 or AlN, and that no correction was made for the amount of Al_2O_3 gained during milling with the used alumina ball-mill medium. Thus, the overall compositions might have deviated from the β-sialon line in the Si–Al–O–N phase diagram towards the two-phase region containing a Si–Al–O–N liquid at the sintering temperature. This would have assisted the densification, and upon cooling the materials would have contained some residual glassy phase, not easily detected by X-ray diffraction.

Studies on the pressureless-sintering behaviour of β-sialon mixtures have also been made by others [19, 20]. It was found by Boskovic and co-workers [19] that near full-density ceramics were obtained only for a β-sialon with $z = 4$ from $Al_2O_3/AlN/Si_3N_4$ mixtures at a very high temperature (1950° C). For lower z-values or lower temperatures the density achieved was significantly lower. Thus at 1800° C these authors found that the β-sialon materials with $z = 2$ and 4 reached only about 92 and 96% TD, respectively. The sensitivity of the densification of β-sialon ceramics to small changes in the overall powder composition was also demonstrated by Rahaman and colleagues [20]. They came to the conclusion that powder compositions corresponding exactly to the β-sialon line in the Si–Al–O–N phase diagram and containing initially very small quantities of a liquid phase, cannot be pressurelessly densified to acceptable levels. Bandyopadhyay and Mukerji [21] have recently shown that a combination of a small excess of SiO_2 in the samples and embedding the samples in an Si_3N_4–SiO_2 mixture, producing SiO vapour, will benefit the densification. Sintering at 1800° C gave sialons with $z = 1.0$ and $z = 2.0$, with densities of 99.7% TD and 98.1% TD, respectively. Finally, it can be mentioned that gas-pressure sintered sialon mixtures (up to 4 MPa nitrogen) at 1800 to 2000° C reached a maximum of 99% TD [6].

Considering the previously reported poor sintering of carefully balanced sialon powder mixtures, the low densities found in this study for the 'pressureless' sintering are to be expected. The use of the glass-encapsulated HIP-technique, however, has proved to be an exellent method for the fabrication of single-phase β-sialon ceramics. With this method, ceramic components of complex shapes can be made directly, reducing the extensive diamond grinding costs otherwise incurred.

The X-ray diffraction analysis of HIP-sintered materials showed that the upper composition limit of the $Si_{6-z}Al_zO_zN_{8-z}$ solid solution at the sintering temperature, 1825° C, and 200 MPa pressure, is slightly lower than 4, about $z = 3.85$. Lumby and co-workers [22] have shown that the homogeneity range of β-sialon at a temperature of 1760° C and at atmospheric pressure of nitrogen extends to 4.2. The two findings are not in good agreement with each other. It is not known to us if the extension range might shift with preparation temperature, but the major cause is probably the high pressure used in the HIP preparations. The preparations made at a low pressure in this study clearly indicated that the extension was up to about 4.1, in fair agreement with Lumby and co-workers [22]. Finally, it can also be seen in Table III that the extra phases observed for z-values $\geqslant 4$ are somewhat different with and without additional sintering aid (1 wt % Y_2O_3). This indicates that there is a small difference in the sintering mechanism, probably due to the larger amount of liquid phase present at high temperature. The liquid facilitates the diffusion and affects also the microstructure by grain coarsening, as shown above.

Determinations of the lattice parameters of β-sialon by XRD techniques have in the past been reported in a number of publications. The findings in the present study are compared with those of Refs 23–26 in Fig. 9. Land and co-workers [23] report a linear variation, the dashed line in Fig. 9, that closely agrees with our results; and Haviar and Johannesen [26] also report a linear shift, the dotted line in Fig. 9. Both these sets of linear data fall within the error limits of the calculated line for our data. The data given for β-Si_3N_4, i.e. $z = 0$, are omitted from the figure for clarity but are reported to be $a = 0.7603$ nm and $c = 0.2909$ nm [23]; $a = 0.7601$ nm and $c = 0.2906$ nm [24, 25]; $a = 0.7603$ nm and $c = 0.2909$ nm [26]; $a = 0.7595$ nm and $c = 0.2902$ [27]; $a = 0.7606$ nm and $c = 0.2911$ nm [28]; which can be compared with our results $a = 0.7603$ nm and $c = 0.2907$ nm.

Greil and Weiss [29] have prepared β-sialon ceramics, with controlled amounts of excess oxygen present in the starting composition, by hot-pressing at 1770° C. In this way they obtained a material containing β-sialon crystals and a variable amount of a Si–Al–O–N amorphous phase. The z-value of the β-sialon phase was not determined, but from the overall composition in the Si–Al–O–N phase diagram it is estimated to be about $z = 0.6$. The microstructure of the sintered materials was carefully studied by TEM techniques and the findings are in fair agreement with our observations on the low z sialon materials. Greil and Weiss found that the materials without excess oxygen, i.e. without amorphous intergranular phase, had a more isotropic crystal shape, whereas increasing the amount of amorphous phase form about 2 to 8 vol % gave a more elongated prismatic grain morphology. This is in concordance with our findings when 1 wt % Y_2O_3 was added to the low z sialon materials, but the effects were not as pronounced in our case, probably because the amount of intergranular phase was much less in our materials.

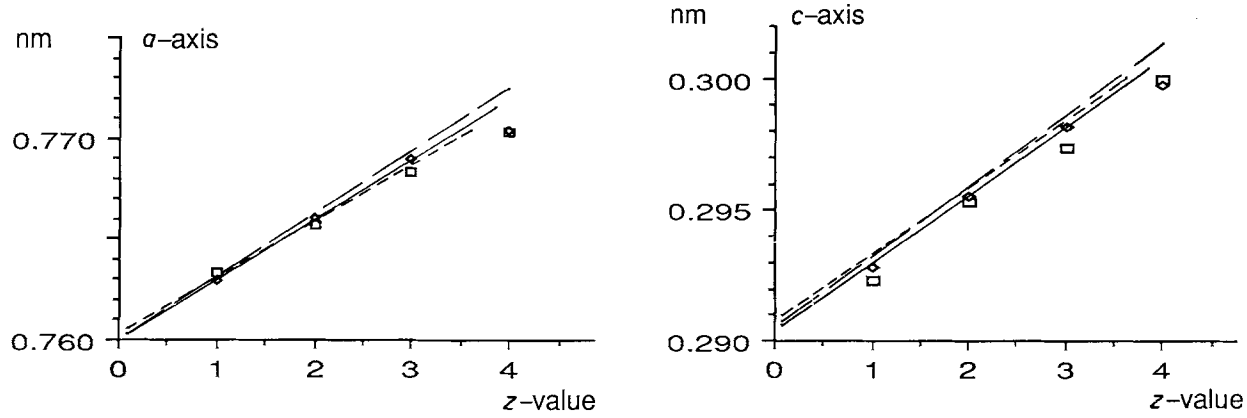

Figure 9 A comparison of the hexagonal lattice parameters of the β-sialon phase obtained by various authors, see text.(□) ref. [24], (◇) ref. 25, (——) our findings (— —) ref. [23], (- - -) ref. [26].

The Vickers microhardness of β-Si_3N_4 single crystals has been measured with a 500 g load to be nearly 2000 [30]. It is expected that the hardness measured on polycrystalline β-Si_3N_4 materials will be somewhat lower. The hardness recorded for the β-sialon material with the lowest z-value = 0.25 was $HV1$ = 1930 (1000 g load) and $HV10$ = 1720 (10 000 g load), which seems reasonable in comparison with the β-Si_3N_4 single-crystal data. The observed hardness decreases as the z-value increases and the substituted β-Si_3N_4 lattice expands, and especially as the grain size increases, see Fig. 7. This behaviour was also observed by Briggs [3], who found that the Vickers microhardness (with a load of 100 g) decreased from 1724 at z = 1 to 1526 at z = 4. On the other hand, a slight increase in hardness with increasing z has been noted for β-sialon/glass materials [18, 31]. However, here other factors might have an influence, such as the amount of glass and its composition.

The fracture toughness at room temperature of the single-phase β-sialon ceramics with low z-values is about 3, similar to dense Si_3N_4 ceramics, but it decreases with increasing z-value, i.e. the materials become more brittle. As shown above, the materials also become softer, mainly because of grain coarsening. For the use as an engineering ceramic at low temperatures, this is not very encouraging, as it indicates lower wear resistance and toughness at higher z-values.

The addition of only 1 wt % Y_2O_3 clearly improved the fracture toughness of the β-sialon ceramics. The reason for this might be that the liquid formed at the sintering temperature aided grain growth and allowed the β-sialon crystals to grow in a more elongated shape. However, the presence of even a small amount of a glassy intergranular phase might adversely affect the high temperature mechanical properties or the oxidation resistance.

5. Conclusions

1. Glass-encapsulated HIP on carefully balanced powder mixtures has proved to be an effective fabrication technique for obtaining single-phase β-sialon ceramics, without residual glassy grain-boundary phase and of virtually theoretical density.

2. Single-phase β-sialon ceramics of low z-values have hardness and fracture toughness similar to those of dense β-Si_3N_4 ceramics. These properties deteriorate with increase of z above 1.

3. The upper limit of the β-sialon solid solution range, $Si_{6-z}Al_zO_zN_{8-z}$, at 1825° C seems to be about z = 3.85 at 200 MPa pressure and about 4.1 at atmospheric pressure.

4. Addition of 1 wt % Y_2O_3 to the β-sialon ceramics prior to sintering causes an amorphous intergranular phase to form, changes the grain size and shape, and gives a clear rise in fracture toughness and a moderate decrease in hardness.

Acknowledgements

AB Sandvik Hard Materials are thanked for permission to publish this article. This work has in part been financed by the Swedish Board for Technical Development.

References

1. K. H. JACK and W. I. WILSON, *Nature Phys. Sci.* **238** (1972) 28.
2. Y. OYAMA and O. KAMIGAITO, *Jpn J. Appl. Phys.* **10** (1971) 1637.
3. J. BRIGGS, *Mater. Res. Bull.* **12** (1977) 1047.
4. M. N. RAHAMAN, F. L. RILEY and R. J. BROOK, *J. Mater. Sci.* **16** (1981) 660.
5. S. UMEBAYASHI, K. KISHI, E. TANI and K. KOBAYASHI, *Yogyo Kyokai Shi* **92** (1984) 35.
6. E. TANI, H. ICHINOSE, K. KISHI, S. UMEBAYASHI and K. KOBAYASHI, *ibid.* **92** (1984) 675.
7. M. N. RAHAMAN, Y. BOITEUX and L. C. DE JONGHE, *Amer. Ceram. Soc. Bull.* **65** (1986) 1171.
8. M. H. LEWIS, B. D. POWELL, P. DREW, R. J. LUMBY, B. NORTH and A. J. TAYLOR, *J. Mater. Sci.* **12** (1977) 61.
9. Y. MIYAMOTO, K. TANAKA, M. SHIMADA and M. KOIZUMI, in "Ceramic Materials and Components for Engines", edited by W. Bunk and H. Hausner (Deutsche Keramische Gesellschaft, Lübeck-Travemünde, 1986) p. 271.
10. N. INGELSTRÖM and T. EKSTRÖM, Proceedings of International Conference on Hot Isostatic Pressing, Luleå, Sweden, 15–16 June 1987 (Centek, Sweden, 1988).
11. H. LARKER, in "Progress in Nitrogen Ceramics", edited by F. L. Riley (Martinus Nijhoff, The Hague, 1983) p. 717.
12. M. MITOMO, N. KURAMOTO and H. SUZUKI, Proceedings of International Symposium on Factors in Densification and Sintering of Oxides and Non-Oxide Ceramics, Japan 1978, p. 463.
13 G. R. ANSTIS, P. CHANTIKUL, B. R. LAWN and D. B. MARSHALL, *J. Amer. Ceram. Soc.* **64** (1981) 533.

14. C. CHATFIELD and H. NORSTRÖM, *ibid.* **66** (1983) C-168.
15. F. K. VAN DIJEN, R. METSELAAR, R. B. HELMHOLDT, *J. Mater. Sci. Lett.* **6** (1987) 1101.
16. M. A. O'KEEFE, in "Electron Optical Systems for Microscopy, Microanalysis and Microlithography", edited by J. J. Hren, F. A. Lenz, E. Munro and P. B. Sewer, 1984 (SEM Inc., Illinois, 1984).
17. C. CHATFIELD, T. EKSTRÖM and M. MIKUS, *J. Mater. Sci.* **21** (1986) 2297.
18. P. O. OLSSON, to be published.
19. S. BOSKOVIC, L. J. GAUCKLER, G. PETZOW and T. Y. TIEN, in "Sintering Processes", edited by G. C. Kuczynski (Plenum Press, London, 1980) p. 295.
20. M. N. RAHAMAN, F. L. RILEY and R. J. BROOK, *J. Mater. Sci.* **16** (1981) 660.
21. S. BANDYOPADHYAY and J. MUKERJI, *J. Amer. Ceram. Soc.* **79** (1987) C-273.
22. R. J. LUMBY, B. NORTH and A. TAYLER, *Spec. Ceramics* **6** (1975) 283.
23. P. L. LAND, J. M. WIMMER, R. W. BURNS and N. S. CHOUDBURY, *J. Amer. Ceram. Soc.* **61** (1978) 56.
24. A. TAKASE, S. UMEBAYASHI and K. KISHI, *J. Mater. Sci. Letters* **1** (1982) 529.
25. A. TAKASE and E. TANI, *ibid.* **3** (1984) 1058.
26. JCPDS XRD-card No. 9-259 (The American Society for Testing Materials).
27. R. GRUN, *Acta Cryst.* **B35** (1979) 800.
28. M. HAVIAR and O. JOHANNESEN, *Adv. Ceram. Mater.* **3** (1988) 405.
29. P. GREIL and J. WEISS, *J. Mater. Sci.* **17** (1982) 1571.
30. D. CHAKRABORTY and J. MUKERJI, *ibid.* **15** (1980) 3051.
31. R. J. LUMBY, *J. Mater. Sci. Lett.* **2** (1983) 345.

Received 4 March
and accepted 25 July 1988